Measurements of the ^{86}Kr$(n,\gamma)^{87}$Kr and ^{86}Kr$(n,2n)^{85}$Kr^m reaction cross sections below $E_n = 15$ MeV

Megha Bhike,[1,2,*] E. Rubino,[3,†] M. E. Gooden,[4,‡] Krishichayan,[1,2] and W. Tornow[1,2]
[1]*Department of Physics, Duke University, Durham, North Carolina 27708, USA*
[2]*Triangle Universities Nuclear Laboratory, Durham, North Carolina 27708, USA*
[3]*Florida Atlantic University, Boca Raton, Florida 33431, USA*
[4]*Department of Physics, North Carolina State University, Raleigh, North Carolina 27695, USA*
(Received 13 May 2015; revised manuscript received 15 June 2015; published 27 July 2015)

The ^{86}Kr$(n,\gamma)^{87}$Kr neutron-capture cross section was measured at 11 energies between 0.37 and 14.8 MeV. Cross-section data for the ^{86}Kr$(n,2n)^{85}$Kr^m reaction were obtained at 9 energies between 10.9 and 14.8 MeV. The data are important for testing calculations used to predict the *s*-process cross section in the unmeasured energy range above 1 MeV for the ^{86}Kr$(n,\gamma)^{87}$Kr reaction, and to check on the consistency of parameters used in TALYS calculations for the ^{86}Kr$(\gamma,n)^{85}$Kr^{m+g} cross section. The two data sets could also be used as a nuclear physics based diagnostic tool for studying properties of the deuterium-tritium plasma created in inertial confinement fusion reactions at the National Ignition Facility at Lawrence Livermore National Laboratory.

DOI: 10.1103/PhysRevC.92.014624 PACS number(s): 26.20.Kn, 25.40.Fq, 25.40.Lw, 52.57.−z

I. INTRODUCTION

Asymptotic giant branch (AGB) stars are assumed to be the source of approximately half of all chemical elements beyond iron in our galaxy [1,2]. These elements are produced via the slow neutron-capture process (*s* process) at relatively low neutron densities. Short-lived radioactive nuclei produced by the *s* process undergo β decay rather than a subsequent neutron capture. However, when the *s* process produces longer-lived isotopes, neutron capture may compete with β decay, giving rise to so-called *s*-process branchings. An important branching point is ^{85}Kr.

Because the ground state of ^{85}Kr β decays with $T_{1/2} = 10.75$ yr, direct measurements of the ^{85}Kr$(n,\gamma)^{86}$Kr neutron-capture cross section above thermal energies do not exist. Recently, Raut *et al.* [3] deduced the ^{85}Kr$(n,\gamma)^{86}$Kr cross section up to 10 MeV neutron energy from measurements of the ^{86}Kr$(\gamma,\gamma')^{86}$Kr cross section between 4.5 and 10 MeV [4] and the ^{86}Kr$(\gamma,n)^{85}$Kr cross sections in the 10 to 13 MeV γ-ray energy range [3]. With this information at hand, the production rate of ^{87}Kr via the *s* process on ^{86}Kr can be calculated, if the neutron-capture cross section on this stable $N = 50$ nucleus is known. Unfortunately, between 200 keV and 1 MeV neutron energy only a single datum exists for the ^{86}Kr$(n,\gamma)^{87}$Kr capture cross section to guide model calculations from the keV to the MeV energy range [5]. In order to improve the (n,γ) database for ^{86}Kr, the neutron-capture cross section was measured between 0.37 and 14.8 MeV at 11 energies. The reaction ^{86}Kr$(n,2n)^{85}$Kr measured in the present work produces the same daughter nucleus as the reaction ^{86}Kr$(\gamma,n)^{85}$Kr studied in [3]. Therefore, it provides an interesting test case of how well the TALYS calculations of [3] for the ^{86}Kr$(\gamma,n)^{85}$Kr^{m+g} reaction reproduce the measured ^{86}Kr$(n,2n)^{85}$Kr^m cross-section data, which previously existed only at 14 MeV.

In addition to the ^{124,136}Xe$(n,\gamma)^{125,137}$Xe and ^{124,136}Xe$(n,2n)^{123,135}$Xe reactions, krypton isotopes have also been considered as dopants in deuterium-tritium (DT) capsules used in laser shots at the National Ignition Facility (NIF) to obtain information on the DT plasma produced in inertial confinement fusion [6]. A sophisticated apparatus has been commissioned at NIF to collect noble gases after a laser shot and to measure the induced activity [7]. The ^{87}Kr activity probes the down-scattered (low-energy) neutron component, while the ^{85}Kr activity from the $(n,2n)$ reaction with its threshold of 10 MeV measures the primary 14.1 MeV DT neutron component, providing, among other characteristics, information on the density of the DT plasma. In order to guarantee a reliable interpretation of such data, the cross sections of interest were measured in the present work.

II. EXPERIMENTAL PROCEDURE, ANALYSIS AND RESULTS

The experimental setup is identical to the one described in Ref. [8]. Briefly, monoenergetic neutrons are produced via the ^{3}H$(p,n)^3$He, ^{2}H$(d,n)^3$He, and ^{3}H$(d,n)^4$He reactions with charged-particle beam currents of 1.5 to 3 μA delivered by the tandem accelerator at Triangle Universities Nuclear Laboratory (TUNL). Krypton gas of mass 1.013 g and enriched to 99.4% in ^{86}Kr is contained in a 20 mm inner diameter stainless steel sphere of 0.5 mm wall thickness. It is positioned at a distance of typically 19 mm from the tritiated titanium target used for neutron energies below 4 MeV and at 14.8 MeV, and at 25 mm from the center of the deuterium gas cell employed to produce neutrons in the 4 to 14.5 MeV energy range. An identical, but empty sphere is used to perform background checks. A photograph of the spheres is shown in Fig. 1. Circular monitor foils of 19 mm diameter and thickness of 0.125 mm were attached to the front and back face of the sphere for neutron fluence determination. Indium

*megha@tunl.duke.edu
†NSF REU 2014 summer student at TUNL.
‡Present address: Nuclear and Radiochemistry Division, Los Alamos National Laboratory, Los Alamos, New Mexico 87545, USA.

FIG. 1. (Color online) Photograph of the high-pressure spheres used in the present work.

foils were used at the lower energies, while gold foils were used for neuron energies above 10 MeV. The entire sphere-monitor foil assembly was surrounded by a thin-walled cage made of cadmium to prevent room-return thermal neutrons from interacting with ^{86}Kr or the monitor foils. The neutron activation technique was applied for both ^{86}Kr and the monitor isotopes ^{115} In and ^{197}Au.

A. The ^{86}Kr$(n,\gamma)^{87}$Kr reaction

After neutron capture on ^{86}Kr, the resulting ground state of ^{87}Kr β decays to ^{87}Rb with $T_{1/2} = 76.3$ min. As can be seen from Fig. 2, the 402.6 keV state in ^{87}Rb with a 41% β-decay transition strength provides a convenient γ ray for determining the ^{86}Kr$(n,\gamma)^{87}$Kr capture cross section. The neutron irradiation time was typically 3 hours, corresponding to approximately 80% saturation. After irradiation, the ^{86}Kr filled sphere and associated monitor foils were γ-ray counted in TUNL's low-background counting facility using 60% (relative efficiency with respect to a 3 inch × 3 inch NaI detector) high-purity germanium (HPGe) detectors surrounded

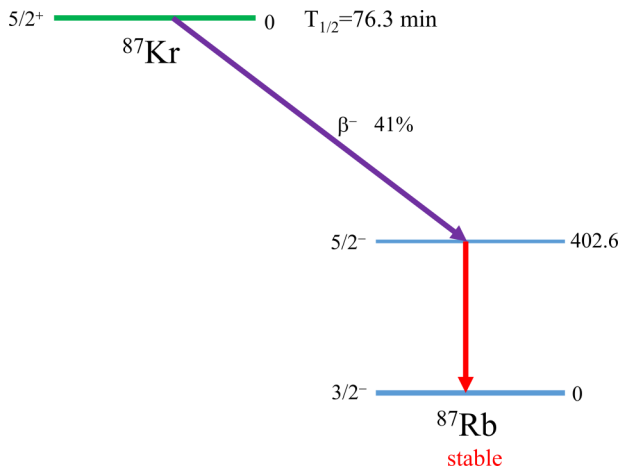

FIG. 2. (Color online) Partial level scheme relevant to the ^{86}Kr$(n,\gamma)^{87}$Kr reaction. All energies are given in keV. Data taken from [9].

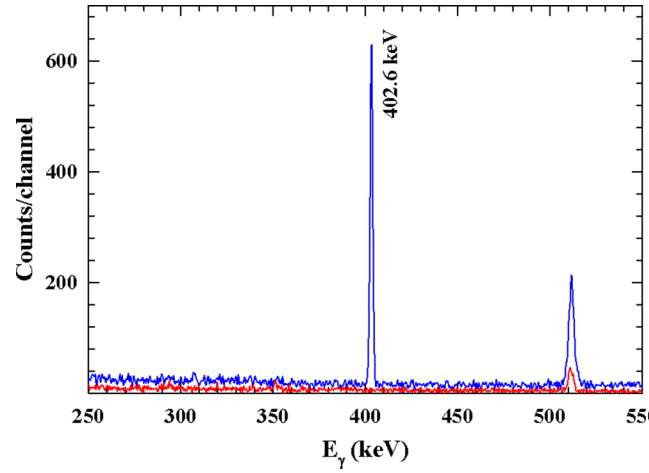

FIG. 3. (Color online) Gamma-ray energy spectra obtained with a HPGe detector. The γ-ray transition of interest for the ^{86}Kr$(n,\gamma)^{87}$Kr cross-section measurement is at 402.6 keV. The spectrum measured with the empty cell is shown for comparison. The neutron energy is $E_n = 1.86$ MeV.

by an enclosure made of lead walls. The center of the sphere was positioned at a distance of 5 cm from the front face of the detector. Using standard data-acquisition electronics [10] the induced γ-ray activity was recorded for a total of typically five hours in up to 10 individual subsets of data. A γ-ray spectrum zoomed-in on the energy region of interest is shown in Fig. 3. It clearly shows the strong 402.6 keV peak and the unavoidable 511 keV peak to the right. Also shown is the energy spectrum recorded with the empty sphere, clearly indicating that there is no contamination hiding under the peak of interest. A calibrated, mixed γ-ray source containing isotopes with energies ranging from 59.5 keV (^{241}Am) to 1836.1 keV (^{88}Y) was used for determining the efficiency of the HPGe detectors employed in the present work. A typical efficiency curve is shown in Fig. 4. At neutron energies of 0.37 and 0.86 MeV the neutron fluence was obtained from

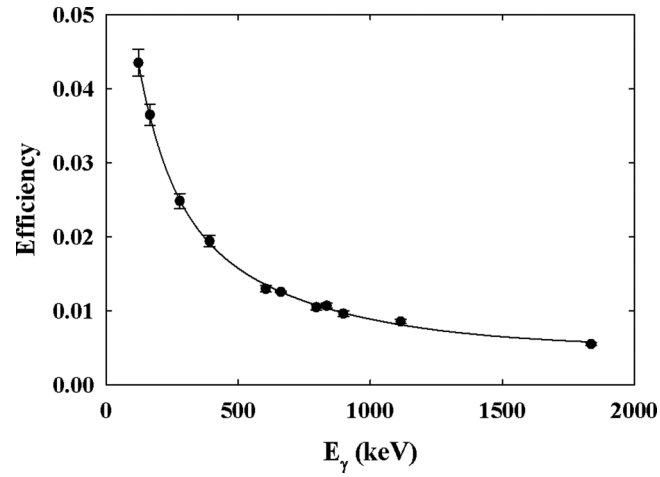

FIG. 4. Measured efficiency data and fit using a mixed γ-ray source positioned at 5 cm from the front face of a 60% relative efficiency HPGe detector.

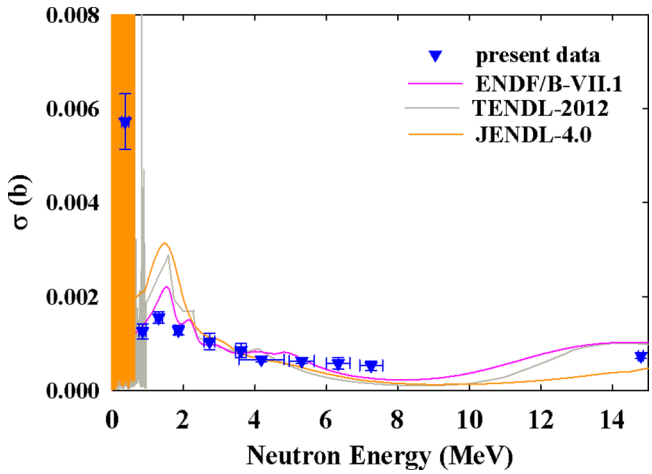

FIG. 5. (Color online) ^{86}Kr$(n,\gamma)^{87}$Kr cross-section data obtained in the present work in comparison to the evaluations ENDF-B/VII.1 and JENDL-4.0 and the model prediction TENDL-2012. The shaded region below 0.7 MeV represents the cross section in the resonance region of the JENDL-4.0 evaluation while slightly above this energy the shaded region up to approximately 1 MeV indicates the cross section predicted by the TENDL-2012 calculation.

the ^{115}In$(n,\gamma)^{116m1}$In reaction with its half-life time of $T_{1/2} =$ 54.29 min and deexcitation γ-ray energy $E_\gamma = 1293.56$ keV and intensity $I_\gamma = 84.8\%$ [11,12]. The ^{197}Au$(n,2n)^{196}$Au reaction with $T_{1/2} = 6.17$ d, $E_\gamma = 355.73$ keV and $I_\gamma = 87\%$ was used at 14.8 MeV [13]. At the neutron energies in between the neutron fluence was determined from the reaction ^{115}In$(n,n')^{115m}$In with $T_{1/2} = 4.49$ h, $E_\gamma = 336.24$ keV, and $I_\gamma = 45.8\%$ [14]. In the latter two cases the data-acquisition time was restricted to eight hours, providing in all cases at least 15000 events in the energy region of interest. After determining the γ-ray yields, small corrections were applied for γ-ray attenuation in the ^{86}Kr sphere and the monitor foils. In addition, corrections were needed to account for geometry differences between the calibration source and the ^{86}Kr sphere and monitor foils. The associated correction factors were obtained from Monte Carlo simulations. The neutron fluence was determined from the activation formula [15] by using the deduced initial activity of the monitor foils, the known cross sections and the other parameters entering into the activation formula. Monte Carlo calculations were also performed to deduce the neutron fluence seen by the ^{86}Kr gas from that obtained from the monitor foils. Finally, the activation formula was employed once more, but this time with the deduced initial activity of ^{86}Kr, the neutron fluences determined above, and the other parameters relevant to ^{86}Kr to obtain the cross-section data of interest.

As has been described in Ref. [16], auxiliary measurements were performed with an untritiated target at nominal neutron energies of 2.73 and 3.61 MeV to account for so-called off-energy neutrons produced by the incident proton beam in the titanium layer and its copper backing. The corrections were 20% and 40%, respectively. Auxiliary measurements were also done at the nominal energies of 6.33 and 7.25 MeV with an empty deuterium gas cell to correct for off-energy neutron contributions created by deuteron-breakup reactions on the structural materials of the gas cell. The associated corrections did not exceed the 5% level.

TABLE I. ^{86}Kr$(n,\gamma)^{87}$Kr reaction: Neutron energy and associated energy spread, monitor reaction cross section used for determining the neutron fluence, and cross-section results for the reaction of interest.

Neutron energy $E_n \pm \Delta E_n$ (MeV)	Monitor reactions σ (mb)	^{86}Kr$(n,\gamma)^{87}$Kr σ (mb)
0.37 ± 0.10	183.90 ± 8.90	5.72 ± 0.59
0.86 ± 0.10	166.44 ± 15.33	1.26 ± 0.16
1.31 ± 0.10	130.23 ± 3.13	1.55 ± 0.12
1.86 ± 0.10	229.72 ± 5.50	1.28 ± 0.10
2.73 ± 0.15	344.50 ± 8.10	1.04 ± 0.17
3.61 ± 0.15	331.59 ± 8.92	0.85 ± 0.15
4.18 ± 0.63	316.02 ± 7.43	0.66 ± 0.05
5.31 ± 0.35	334.57 ± 8.70	0.63 ± 0.05
6.33 ± 0.33	346.09 ± 12.30	0.58 ± 0.12
7.25 ± 0.32	323.22 ± 11.50	0.53 ± 0.10
14.80 ± 0.07	2164.20 ± 22.83	0.74 ± 0.06

Results for the ^{86}Kr$(n,\gamma)^{87}$Kr neutron-capture cross section are shown in Fig. 5 in comparison to predictions based on the evaluations ENDF/B-VII.1 [17] and JENDL-4.0 [18], and the model prediction TENDL-2012 [19] of the TALYS code. As pointed out already, the previous data were limited to neutron energies below 200 keV and to a single datum at 1 MeV. The present data reproduce the trend of the evaluations fairly well, but do not support the magnitude of the strong cross-section enhancement predicted at $E_n = 1.5$ MeV. It should also be noted that our datum in the resonance region at 0.37 MeV favors the trend of the datum of Walter *et al.* [20] over the work of Beer *et al.* [21] at energies below 200 keV. We do not have an explanation why Hauser-Feshbach calculations [21] provide a consistently smaller value, unless nonstatistical contributions play a significant role in the 0.37 MeV energy region. Table I gives our results in numerical form, while Table II provides the uncertainty budget of the present cross-section data.

TABLE II. Uncertainty budget for ^{86}Kr$(n,\gamma)^{87}$Kr and monitor reaction cross-section data.

Uncertainty	Kr(%)	Monitors(%)
Counting statistics	1.5–16.5	0.1–10.3
Reference cross sections		1–9.2
Neutron flux correction		<2
Detector efficiency	3.20–3.57	0.96–4.93
Source geometry and self-absorption of γ-ray	<0.2	<0.2
Half-life	< 1	< 0.31
γ-ray intensity	6	1.42–4.80
Neutron flux fluctuation	<1	< 1
Lower-energy neutrons	<5	<1.5

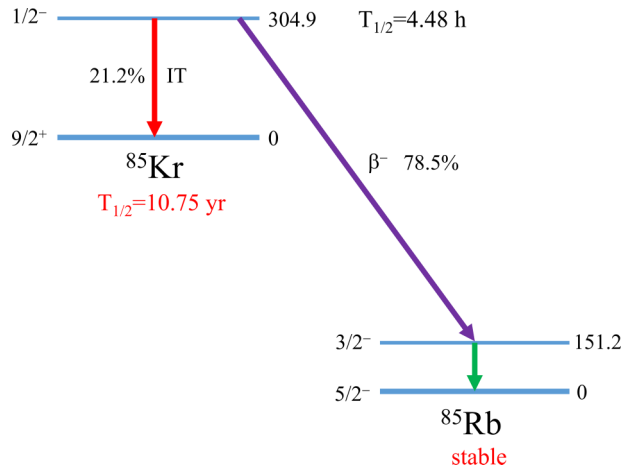

FIG. 6. (Color online) Partial level scheme relevant to the ^{86}Kr$(n,2n)^{85}$Kr^m reaction. All energies are given in keV. Data taken from [9].

B. The ^{86}Kr$(n,2n)^{85}$Kr^m reaction

A partial level scheme of ^{85}Kr and its β-decay daughter ^{85}Rb is shown in Fig. 6. The ^{86}Kr$(n,2n)^{85}$Kr reaction populates the isomeric state of ^{85}Kr at 304.9 keV, which either decays via an isomeric transition IT to its ground state with $T_{1/2} =$ 4.48 h and branching ratio of 21.2%, or via β decay to ^{85}Rb with a branching ratio of 78.5%. The ground state of ^{85}Kr in turn β decays with $T_{1/2} = 10.75$ yr to ^{85}Rb. The decay of the 151.2 keV state in ^{85}Kr provides a convenient γ ray for measuring the ^{86}Kr$(n,2n)^{85}$Kr^m cross section to the isomeric state of ^{85}Kr.

Because $(n,2n)$ cross sections are approximately three orders of magnitude larger than (n,γ) cross sections in the 10 MeV neutron energy range, irradiation times of two hours are more than sufficient when using the ^{2}H$(d,n)^3$He neutron source reaction. The threshold for initiating the

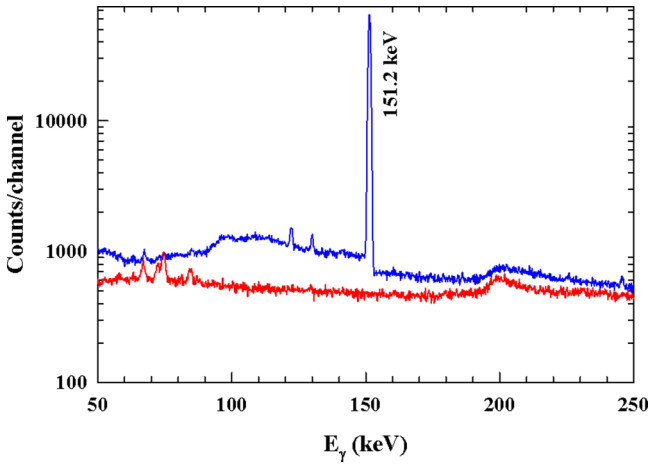

FIG. 7. (Color online) Gamma-ray energy spectrum obtained with a HPGe detector. The γ-ray transition of interest for the ^{86}Kr$(n,2n)^{85}$Kr^m cross-section measurement is at 151.2 keV. The lower spectrum was recorded with the empty sphere after irradiation with 12.5 MeV neutrons.

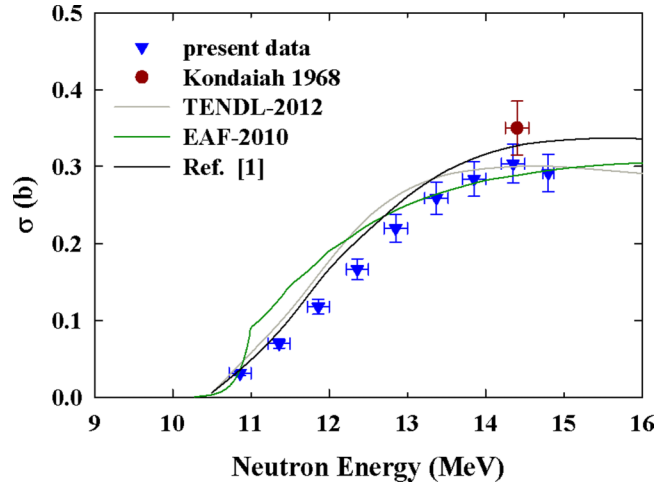

FIG. 8. (Color online) ^{86}Kr$(n,2n)^{85}$Kr^m cross-section data in comparison to the previously existing datum at 14.4 MeV [22], the model calculation TENDL-2012 and the evaluation EAF-2010.

^{86}Kr$(n,2n)^{85}$Kr reaction is 9.972 MeV. Data were taken in 0.5 MeV increments from nominal 10.9 to 14.5 MeV, using the ^{197}Au$(n,2n)^{196}$Au reaction as neutron fluence monitor. With its threshold energy of 8.11 MeV, this reaction is sensitive to deuteron breakup neutrons once the neutron energy of 14 MeV, produced via the ^{2}H$(d,n)^3$He reaction, is surpassed. Therefore, as a cross-check, the ^{3}H$(d,n)^4$He reaction was used to produce 14.8 MeV neutrons.

The experimental arrangement was very similar to that used for the ^{86}Kr$(n,\gamma)^{87}$Kr cross-section measurements, except that the cadmium enclosure of the ^{86}Kr sphere was not necessary. A typical γ-ray spectrum zoomed-in on the 151.2 keV line of interest is shown in Fig. 7. This spectrum was obtained with a planar HPGe detector of known efficiency. The data analysis was identical to that described in Sec. II A.

Our results for the ^{86}Kr$(n,2n)^{85}$Kr^m reaction are shown in Fig. 8 in comparison to the previously existing datum near 14 MeV and the results of the evaluation EAF-2010 [23] and the model calculation TENDL-2012 based on the TALYS

TABLE III. ^{86}Kr$(n,2n)^{85}$Kr^m reaction: Neutron energy and associated energy spread, monitor reaction cross section used for determining the neutron fluence, and cross-section results for the reaction of interest.

Neutron energy $E_n \pm \Delta E_n$ (MeV)	Monitor reactions σ(mb)	^{86}Kr$(n,2n)^{85}$Kr^m σ (mb)
10.86 ± 0.14	1401.14 ± 39.23	30.93 ± 2.57
11.36 ± 0.14	1564.05 ± 42.07	69.60 ± 5.78
11.86 ± 0.14	1701.31 ± 44.06	117.56 ± 9.70
12.36 ± 0.14	1823.51 ± 44.68	166.26 ± 13.67
12.85 ± 0.15	1933.86 ± 43.90	219.51 ± 17.93
13.37 ± 0.15	2038.87 ± 37.92	259.00 ± 20.90
13.85 ± 0.15	2114.60 ± 26.43	283.65 ± 22.52
14.35 ± 0.15	2152.99 ± 24.11	303.50 ± 25.19
14.80 ± 0.07	2164.20 ± 22.83	291.15 ± 24.41

TABLE IV. Uncertainty budget for ^{86}Kr$(n,2n)^{85}$Kr^{m} and monitor reaction cross-section data.

Uncertainty	Kr(%)	Monitor(%)
Counting statistics	0.1–0.2	0.4–0.7
Reference cross sections		1–2.8
Neutron flux correction		<2
Detector efficiency	1.5–3.2	3.8
Source geometry and self-absorption of γ-ray	<0.2	<0.2
Half-life	0.18	0.01
γ-ray intensity	0.66	
Neutron flux fluctuation	<1	< 1

code. There is fairly good agreement between the data and the predictions, although the present data are lower in magnitude than the TENDL-2012 calculations in the 12 to 13 MeV energy range. The EAF-2010 evaluation is clearly too low between 11 and 13 MeV. The parameters used in Ref. [3] in the TALYS calculations for the ^{86}Kr$(\gamma,n)^{85}$Kr^{m+g} cross section provide the black curve of Fig. 8, which is also in fair agreement with the present data. Finally, Tables III and IV present our data and the associated uncertainty budget in numerical form.

III. CONCLUSION

For the first time neutron capture cross-section data are reported for ^{86}Kr for energies above 1 MeV. They are in fair agreement with the ENDF/B-VII.1 evaluations and the model calculation TENDL-2012 of the TALYS code. The parameters determined in Ref. [3] for obtaining the ^{85}Kr$(n,\gamma)^{86}$Kr cross section, from the measured ^{86}Kr$(\gamma,\gamma')^{86}$Kr and ^{86}Kr$(\gamma,n)^{85}$Kr data, provide a fair description of the present ^{86}Kr$(n,2n)^{85}$Kr^{m} data, giving confidence in the calculated cross section reported in Ref. [3] for the important branching point reaction ^{85}Kr$(n,\gamma)^{86}$Kr. Our cross-section data also provide a potential and alternative tool for studying the plasma density obtained in internal confinement DT fusion shots at NIF.

ACKNOWLEDGMENTS

We thank Dr. Ronald Schwengner, Technical University Dresden, Germany, for providing the ^{86}Kr filled and empty spheres. The authors also acknowledge valuable contributions from A. P. Tonchev, LLNL, B. Fallin and S. W. Finch, Duke University. This work was supported in part by the US Department of Energy, Office of Nuclear Physics, under Grant No. DE-FG02-97ER41033, and by the National Nuclear Security Administration under the Stewardship Science Academic Alliances Program through the US Department of Energy Grant No. DE-NA0001839.

[1] F. Herwig, Ann. Rev. Astron. Astrophys. **43**, 435 (2005).
[2] M. Busso, R. Gallino, and G. J. Wasserburg, Ann. Rev. Astron. Astrophys. **37**, 239 (1999).
[3] R. Raut *et al.*, Phys. Rev. Lett. **111**, 112501 (2013).
[4] R. Schwengner *et al.*, Phys. Rev. C **87**, 024306 (2013).
[5] D. J. Hughes, R. C. Garth, and J. S. Levin, Phys. Rev. **91**, 1423 (1953).
[6] D. A. Shaughnessy, C. Cerjan, K. J. Moody, L. Bernstein, R. Hoffman, M. A. Stoyer, R. Fortner, and D. Schneider, Lawrence Livermore National Laboratory Report No. LLNL-TR-472959 (2011) (unpublished).
[7] D. A. Shaughnessy, C. A. Velsko, D. R. Jedlovec, C. B. Yeamans, K. J. Moody, E. Tereshatov, W. Stoeffl, and A. Riddle, Rev. Sci. Instrum. **83**, 10D917 (2012).
[8] Megha Bhike, B. Fallin, M. E. Gooden, N. Ludin, and W. Tornow, Phys. Rev. C **91**, 011601(R) (2015).
[9] http://www.nndc.bnl.gov/nudat2/.
[10] http://www.canberra.com.
[11] A. I. Leipunskiy, O. D. Kazachkovskiy, G. Ja. Artyukhov, A. I. Baryshnikov, T. S. Belanova, V. I. Galkov, Yu. Ja. Stavisskiy, E. A. Stumbur, and L. E. Sherman, in *Second International Atomic Energy Conference, Geneva, 1958*, Vol. 15 (IAEA, Vienna, 1958), p. 50.
[12] R. P. Gautam, R. K. Y. Singh, I. A. Rizvi, M. Afzal Ansari, A. K. Chaubey, and S. Kailas, Indian J. Pure Appl. Phys. **28**, 235 (1990).
[13] K. I. Zolotarev *et al.*, INDC(NDS)-526 (2008).
[14] A. B. Smith, S. Chiba, D. L. Smith, J. W. Meadows, P. T. Guenther, R. D. Lawson, and R. J. Howerton, ANL/NDM-115 (1990).
[15] Megha Bhike and W. Tornow, Phys. Rev. C **89**, 031602(R) (2014).
[16] Megha Bhike, B. Fallin, and W. Tornow, Phys. Lett. B **736**, 361 (2014).
[17] M. B. Chadwick *et al.*, Nucl. Data Sheets **112**, 2887 (2011).
[18] K. Shibata *et al.*, Nucl. Sci. Technol. **48**, 1 (2011).
[19] A. J. Koning, S. Hilaire, and M. C. Duijvestijin, in *Proceedings of the International Conference on Nuclear Data for Science and Technology, Santa Fe*, edited by R. C. Haight, M. B. Chadwick, T. Kawano, and P. Talou, AIP Conf. Proc. No. 769 (AIP, New York, 2005), p. 1154.
[20] G. Walter, B. Leugers, F. Kappeler, Z. Y. Bao, G. Reffo, and F. Fabbri, Nucl. Sci. Eng. **93**, 357 (1986).
[21] H. Beer, P. V. Sedyshev, W. Rochow, P. Mohr, and H. Oberhummer, Nucl. Phys. A **705**, 239 (2002).
[22] E. Kondaiah, N. Ranakumar, and R. W. Fink, Nucl. Phys. A **120**, 337 (1968).
[23] J.-Ch Sublet, L. W. Packer, J. Kopecky, R. A. Forrest, A. J. Koning, and D. A. Rochman, The European Activation File: EAF-2010 Neutron-induced Cross Section Library, EASY Documentation Series CCFE-R (10) 05, April 2010.